


Absolute frequency measurement of the $6D_{5/2}$ level of neutral ^{133}Cs using two-photon spectroscopy

M. T. Herd¹, E. C. Cook², and W. D. Williams^{2,*}

¹*Department of Biological and Physical Sciences, Assumption University, Worcester, Massachusetts 01609, USA*

²*Department of Physics, Smith College, Northampton, Massachusetts 01063, USA*

 (Received 11 July 2021; revised 28 September 2021; accepted 29 September 2021; published 19 October 2021)

We report absolute frequency measurements on the $6D_{5/2}$ level of neutral ^{133}Cs using sub-Doppler two-photon spectroscopy. The absolute center-of-gravity energy for the $6D_{5/2}$ level is determined to be $22\,631.683\,877(6)\text{ cm}^{-1}$, a factor of 170 times improvement over the previous measurement from 1964 of $22\,631.6863(10)\text{ cm}^{-1}$. This measurement also corrects a 2.4σ discrepancy with the previously measured value. The hyperfine coefficients were found to be $A = -4.629(14)$ and $B = -0.10(15)$ MHz, which are consistent with previous results.

DOI: [10.1103/PhysRevA.104.042812](https://doi.org/10.1103/PhysRevA.104.042812)

I. INTRODUCTION

Neutral cesium-133 is an important atom in atomic physics. The frequency separation of the two ground-state hyperfine levels defines the second [1,2]. Additionally, there are readily available lasers that can be used to laser cool and trap the element. Properties of the excited states of cesium, such as fine and hyperfine structures and absolute transition frequencies, have been studied extensively. Frequency combs have been used to measure absolute frequencies of a number of transitions including the $6S_{1/2} - 6P_{1/2}$ D1 line [3], the $6S_{1/2} - 6P_{3/2}$ D2 line [4], the $6S_{1/2} - 8S_{1/2}$ two-photon transition [5], and the $6S_{1/2} - 8P_{1/2}$ transition [6], leading to uncertainties on these states as small as 2.4 kHz [3]. Li *et al.* reported high precision measurements on the $8S_{1/2}$, $9S_{1/2}$, and $7D_{3/2}$ states [7]. Deiglmayr *et al.* used a frequency comb for the $nP_{1/2}$ and $nP_{3/2}$ Rydberg states to extract the ionization threshold [8]. Recently, our group measured the absolute transition frequencies for the $7P_{1/2}$ and $7P_{3/2}$ states to better than 1.5-MHz precision using a calibrated ultralow expansion (ULE) cavity as a reference [9].

This paper concerns the $6D_{5/2}$ state in neutral cesium-133. The absolute frequency of the $6D_{5/2}$ and $6D_{3/2}$ states was first measured by Eriksson *et al.* in 1964 to a precision of 30 MHz [10,11]. In 2018, Chen *et al.* performed high-precision spectroscopy on the $6D_{3/2}$ line to a precision of 192 kHz, exploring the potential of this line as a frequency standard [12]. In 2005, Ohtsuka *et al.* explored both the $6D_{5/2}$ and the $6D_{3/2}$ states, but their measurement of the absolute frequency transition did not improve upon Eriksson *et al.* [13].

A number of groups have measured the hyperfine constants for these two $6D$ states. To the best of our knowledge, Chen *et al.* [12], who was also able to extract the magnetic octupole hyperfine constant, reported the lowest uncertainty for the $6D_{3/2}$ hyperfine constants whereas Kortyna *et al.* [14] reported the lowest uncertainty for the $6D_{5/2}$ hyperfine constants, see

Table I for a summary of hyperfine constants for the $6D_{5/2}$ state including the results from this paper. In this paper, we report on the absolute frequency of the $6D_{5/2}$ state by performing two-photon spectroscopy from the ground state, see Fig. 1 for a simplified Grotrian diagram. The values reported here improve the precision of the $6D_{5/2}$ state by a factor of 170 and correct a 2.4σ discrepancy with the Eriksson *et al.* result, which is currently the reported value in the NIST database [15].

The paper is organized as follows: Sec. II describes the experimental setup. Section III presents results and a discussion of the systematic and statistical uncertainties that limit the precision of this experiment. Section IV concludes with a summary of the results.

II. EXPERIMENTAL SETUP

Figure 2 shows the simplified experimental setup. The $6S_{1/2} - 6D_J$ excitation beam is provided by a Verdi-pumped Ti:S laser (MSquared Lasers SolsTiS) with the output roughly collimated using a 500-mm focal length lens to a beam waist of $w_x \times w_y = 600 \times 850\ \mu\text{m}$. A 150-mm focal length lens is used to focus the laser into the room-temperature Cs vapor cell (TRIAD Technologies, Inc. TT-CS-20X75-CW). At the output of the cell, a second 150-mm focal length lens recollimates the beam, which is then retroreflected back through the cell. A half-wave plate ($\lambda/2$) combined with a polarizing beam splitter at the cell input is used to adjust the excitation intensity and dump the retroreflected beam. The measured beam waists at the center of the vapor cell are $w_x \times w_y \sim 45 \times 40\ \mu\text{m}$. The cell is wrapped with four layers of 0.152-mm-thick high-permeability magnetic shielding foil (Thorlabs MSFHP) to minimize background magnetic fields.

Successful excitation is detected by monitoring the subsequent $6P_{3/2} - 6S_{1/2}$ fluorescence at 852 nm, see Fig. 1, using an avalanche photodiode (APD, Thorlabs APD401A). An 850-nm bandpass interference filter (Thorlabs FL850-10) blocks the scattered 884-nm excitation light, the $6D_J - 6P_{3/2}$ fluorescence at 917/922-nm ($J = 5/2, 3/2$), and the $6P_{1/2} -$

*williams@smith.edu

TABLE I. Absolute transition frequencies from the center-of-gravity of the $6S_{1/2}$ ground state to the center-of-gravity of the $6D_{5/2}$ state and the hyperfine constants for the $6D_{5/2}$ state. Spectroscopy was performed from both the $F = 3$ and the $F = 4$ hyperfine levels of the ground state.

Measurement	f_{cog} (MHz)	A (MHz)	B (MHz)
From $F = 4$	678 480 813.81(18)	-4.622(11)	-0.14(12)
From $F = 3$	678 480 813.82(18)	-4.637(16)	-0.06(17)
From $F = 4$ (cm^{-1})	22 631.683 877(6)		
From $F = 3$ (cm^{-1})	22 631.683 877(6)		
Previous work			
Eriksson <i>et al.</i> [10]	678 480 890(30)		
Ohtuka <i>et al.</i> [13]		-4.56(9)	-0.35(18)
Georgiades <i>et al.</i> [21]		-4.69(4)	0.18(73)
Kortana <i>et al.</i> [14]		-4.66(4)	0.9(8)

$6S_{1/2}$ fluorescence at 894 nm. The 852-nm fluorescence is collected via 1:1 imaging using two 25.4-mm focal length lenses, each with a diameter of 25.4 mm. The APD signal is then amplified and sent through a low-pass filter (Stanford Research Systems SRS560) before being recorded by a computer.

For controlled calibrated frequency scans, we reference the frequency-doubled output of the Ti:S at 470 nm to a calibrated temperature-stabilized ULE cavity [16] with a free spectral range of $\Delta\nu = 1.5$ GHz using an offset sideband lock [17–19]. Details of our offset sideband lock can be found in Refs. [18,19]. Briefly, a fiber-coupled EOM (AdvR Inc., WPM-P48P48-AL0-488 nm) with a bandwidth of 6 GHz is driven at 20 MHz and at a variable higher-frequency f_s using a function generator (Stanford Research Systems SG384). The frequency of the laser is controlled and stabilized by Pound-Drever-Hall stabilization [20] using one of the high-frequency sidebands. When stabilized to the negative high-frequency sideband, the frequency of the laser used for the two-photon

excitation is

$$f_L = \frac{1}{2}(f_n + f_s), \quad (1)$$

where f_n is the frequency of the ULE cavity mode and f_s is the high-frequency sideband. The factor of $\frac{1}{2}$ on the right-hand side is due to stabilizing the laser using frequency-doubled light whereas the cesium atoms are probed with the non-frequency doubled light. This technique allows the laser to be scanned in frequency by scanning the frequency of the high-frequency sideband. The frequency of the laser is determined by the frequency comb (Toptica DFC CORE with EXT935), which is referenced to a 10-MHz GPS-disciplined Rb oscillator (Stanford Research Systems FS740). The beat note between the Ti:sapphire laser and the frequency comb f_b is monitored continuously throughout data collection by both the phase-frequency detector of the Toptica system and a separate counter (Stanford Research Systems SRS820). Both counters as well as the function generator driving the EOM are also referenced to the 10-MHz GPS-disciplined oscillator. There is poor resolution on the counters as the beat note approaches 0 or 40 MHz ($f_{\text{rep}}/2$) as higher-order multiples of $\pm f_b$ begin to overlap. A manually tuned digital filter is used to minimize the range where beat frequencies are inaccurate. For those beat frequencies ($f_b < 1$ and $f_b > 35$ MHz), a linear extrapolation is used. A 30-MHz wave meter (High-Finesse/Angstrom WS7-30) is used to verify the comb order n_{comb} for each scan range such that the laser frequency is given by $f_L = n_{\text{comb}}f_{\text{rep}} \pm f_b$. This setup allows for good

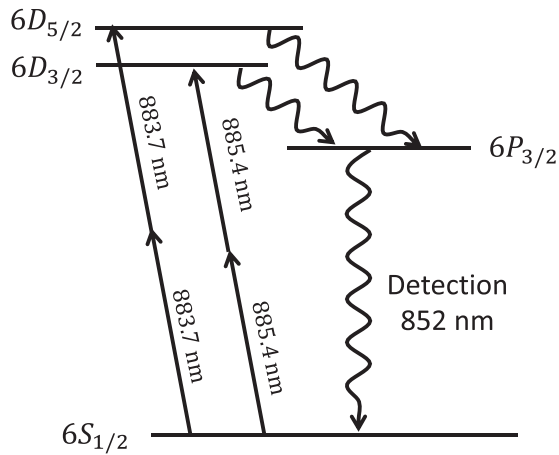


FIG. 1. Simplified Grotrian diagram of neutral cesium-133. We perform two-photon spectroscopy from the $6S_{1/2}$ hyperfine states to the $6D_{5/2}$ state. Detection is performed using 852-nm fluorescence from the $6P_{3/2}$ state. Also included is the $6D_{3/2}$ state, which was used to confirm our setup by reproducing a measurement from Chen *et al.* [12].

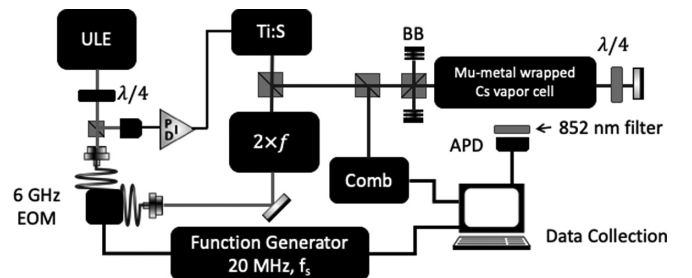


FIG. 2. Simplified experimental setup. Details in the text. Titanium sapphire laser: (Ti:S); frequency doubling cavity: ($2 \times f$); ultralow expansion cavity: (ULE); beam block; (BB); avalanche photodiode: (APD); electro-optical modulator (EOM).

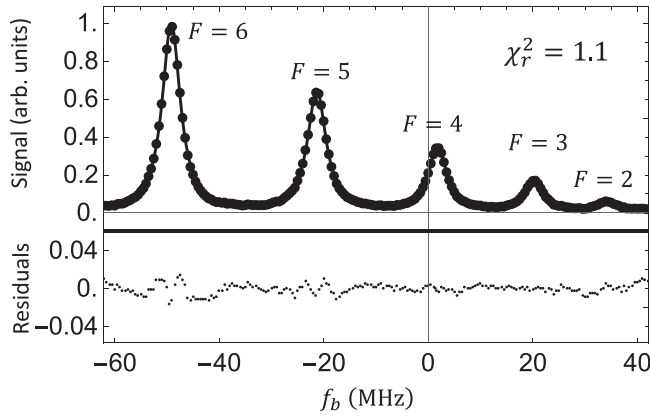


FIG. 3. An example two-photon spectrum from $6S_{1/2} F = 4-6D_{5/2}$ with an input laser power of 250 mW. The spectrum has had a vertical offset removed and was normalized for better visual analysis of the residuals. The experimental data (dots) and the fit (solid line) as described in the text are included in the plot. The reduced χ^2 value χ_r^2 for this fit is 1.1.

frequency stability provided by the ULE cavity with accurate frequency measurements that are independent of residual amplitude modulation (RAM) in the limit of slow RAM drifts compared to the data collection time, which, for us is 100 ms.

III. RESULTS AND DISCUSSION

The Ti:sapphire laser is stabilized to the ULE cavity using the frequency-doubled output as described in Sec. II and scanned across the $6D_{5/2}$ hyperfine spectra by stepping the frequency driving the EOM f_s that determines the ULE cavity sideband frequency with the APD output and the frequency-comb beat note f_b recorded by a computer. The typical f_s step interval is 0.5 MHz (0.25 MHz in the IR) with a 100-ms settling time used between data points. We average the APD and f_b signals for 100 ms for each data point using a 100-kHz acquisition rate for the APD (averaging 10 000 samples per data point) and a 10-ms gate time for the SR820 f_b frequency measurement. The laser is alternately scanned up and down in frequency across the spectra to look for hysteresis effects; no hysteresis effects were observed. Figure 3 shows a typical $6D_{5/2}$ hyperfine spectra from the $6S_{1/2} F = 4$ state as a function of the frequency-comb beat note. The negative beat note on the horizontal axis of Fig. 3 indicates the laser frequency is lower than the nearest comb mode frequency.

Each recorded spectrum is fit to a sum of five Lorentzians plus an offset. The Hamiltonian that describes a particular hyperfine level is given by

$$H = A(\mathbf{I} \cdot \mathbf{J}) + B \frac{3(\mathbf{I} \cdot \mathbf{J})^2 + (3/2)(\mathbf{I} \cdot \mathbf{J}) - I(I+1)J(J+1)}{2I(2I-1)J(2J-1)}, \quad (2)$$

which leads to a hyperfine energy splitting from the center of gravity given by

$$\Delta E = \frac{1}{2}AK + B \frac{(3/2)K(K+1) - 2I(I+1)J(J+1)}{2I(2I-1)2J(2J-1)}, \quad (3)$$

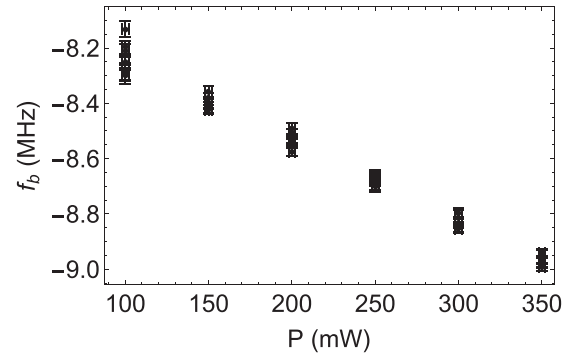


FIG. 4. The center of gravity vs input power repeated over eight data sets extracted from the $6S_{1/2} F = 4-6D_{5/2}$ spectrum. Each set is fit to a linear line to extract the zero power center of gravity frequency.

where $K = F(F+1) - I(I+1) - J(J+1)$, A is the magnetic dipole constant, B is the electric quadrupole constant, I is the nuclear spin, J is the total electronic angular momentum, and F is the total atomic angular momentum for a given hyperfine level. In this equation, the term with the electric quadrupole constant does not appear when $J = 1/2$.

Referring to Eq. (3), the center frequencies of all five Lorentzians are determined using three free parameters: the center of gravity frequency f_{cog} (with respect to f_b), the magnetic dipole hyperfine constant A , and the electric quadrupole hyperfine constant B . The spectrum was fit using *Mathematica*'s `NonlinearModelFit` function. `NonlinearModelFit` assumes that the original data points are independently normally distributed with a common standard deviation. The fit parameters, namely, f_b , A , and B , are returned with uncertainty at the 95% confidence level.

To account for light shifts, the spectra was recorded at laser powers ranging from 100- to 350-mW input power and extrapolated to zero power. To determine the statistical/repeatability uncertainty, data were collected in “runs.” A run consists of spectra using powers ranging from 350 to 100 mW, which included scanning the frequency both up and down at each power to check for hysteresis effects. In this way each data run consists of two data sets across all powers, one for scanning up in frequency and a second from scanning down in frequency. After each data run, the setup was realigned to minimize position drifts of the laser beam. Although position drifts were noticeable on long-time scales, on the order of several hours, position drifts were not seen on the timescales needed for a single data run, about 20 min. Figure 4 shows the center of gravity frequency as measured by f_b as a function of laser power. Each data set is fit to a linear line to extract the zero power center-of-gravity frequency. The linear line was also fit using *Mathematica*'s `NonlinearModelFit` function. Since each f_b for a particular power has an error bar from the previous spectrum fit, we use `NonlinearModelFit` with a variance estimator function of 1 and weight each data point using $1/(\delta f_b)^2$, where δf_b is the uncertainty of f_b . These options indicate that the parameter errors are effectively computed only from the weights.

Figure 5 shows 38 data set extractions and a histogram of the final data from the $6S_{1/2} F = 4$ state to the $6D_{5/2}$

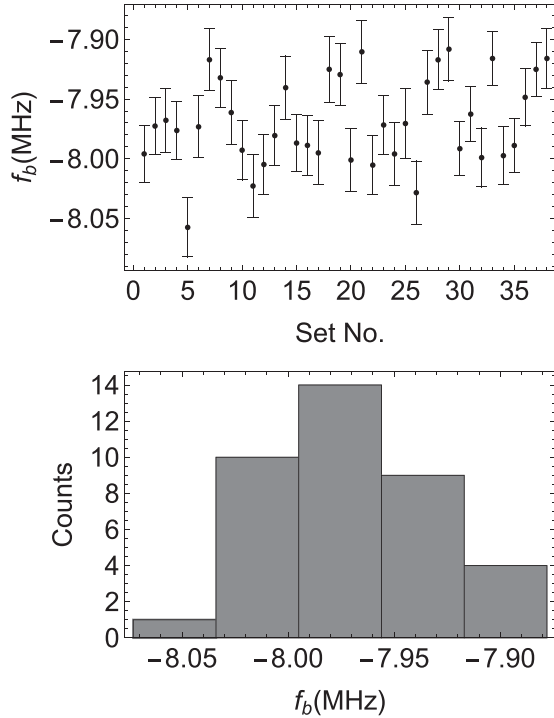


FIG. 5. The center of gravity and histogram at 0 power for 38 data sets, see the text, extracted from the $6S_{1/2} F = 4-6D_{5/2}$ spectrum.

state. The standard deviation of this histogram is used as the repeatability uncertainty. The same procedure was followed for spectra taken from the $6S_{1/2} F = 3-6D_{5/2}$ transition.

Background magnetic fields introduce peak broadening and potential systematic absolute frequency shifts arising from optical pumping. To reduce this systematic effect, a cylindrical μ metal shield consisting of four layers with a 0.8-cm diameter window for APD optical access was wrapped around the cell. The shield was initially tested by measuring the magnetic field inside the μ -metal cylinder with external magnetic fields up to 6.6 G. The internal magnetic field remained at zero to the precision of the magnetic-field probe (Lakeshore MST-410). To further quantify the potential magnetic-field systematic, a pair of Helmholtz coils (7-cm coil radius and coil separation, 168 turns per coil) were used to provide a uniform magnetic field. Spectra were taken in uniform magnetic fields ranging from -6.6 to $+6.6$ G. No shift in the spectrum is observed within the repeatability of the experiment allowing us to conclude that any effects due to residual magnetic fields are negligible compared to the statistical and repeatability uncertainty of the data.

An error due to the alignment of the retroreflected beam not being directed on top of the incident beam was estimated using the procedure outlined by Wu *et al.* [22]. With a fixed input laser power of 350 mW, the retroreflected beam was purposely misaligned until the signal dropped by 50%. Three data runs using this method were completed and a small average offset of 86 kHz was found. Since any misalignment of the actual experiment was significantly less than 50% signal reduction, we, conservatively, take the uncertainty due to laser misalignment to be 8.6 kHz.

TABLE II. Systematic and statistical measurement uncertainties (one standard deviation) for the absolute energy of the $6D_{5/2}$ state.

	Uncertainty (kHz)
B field	Negligible
Possible pressure shifts	175
Repeatability	37
Comb	1.4
Alignment	8.6
Power	4
Overall	180

Extracting to zero power is an important aspect of our measurement and relies on accurate measures of power. The power meter was very sensitive to alignment, and care was taken to check repeatably by measuring the power after each run. We assume that we were always within 1.0 mW of the actual power reading. This gives an error of 3.1 kHz on the extracted zero power center of gravity frequency. We also applied a random normal distribution with a standard deviation of 2 mW around each power during analysis. This variation represents how close we got to each power setting. The average f_{cog} did not change due to this analysis, but the uncertainty increased by 2.5 kHz, which gives a total uncertainty due to the power measurement of 4 kHz.

Gas diffusion into glass cells can lead to broadening of the lines and a shift in peak frequency [23]. Our vapor cell is a sealed cell that has an unknown internal pressure. To account for possible frequency shifts due to gas leakage or background pressure, we measured the nearby $6S_{1/2}$, $F = 4-6D_{3/2}$, $F = 5$ transition and compared the result to those obtained by Chen *et al.* using an ultra-high-vacuum (UHV) cell [12]. The result of Chen *et al.* [12], which is 677 191 794 262(192) kHz, is consistent with our measurement which, without a possible pressure shift correction, is 677 191 794 437(38) kHz. The discrepancy between the two measurements is 175 kHz and a pressure shift in our cell would increase the measured transition frequency. We, therefore, conservatively include a 175-kHz uncertainty due to this systematic. A future study performed in an UHV environment can remove this uncertainty to provide a higher precision measurement.

The 2018 measurement of Chen *et al.* [12] has a 2.9σ discrepancy with the reported value of Eriksson *et al.* for the $6S_{1/2} - 6D_{3/2}$ transition [10], similar to the 2.4σ discrepancy we are reporting here. Note in both cases the updated measurements are lower than the reported values of Eriksson *et al.* [10].

Finally, the frequency-comb accuracy contributes an uncertainty of less than <700 Hz (1 part in 10^{11}). The comb uncertainty is multiplied by 2 since we are reporting on the absolute frequency of the transition and not the frequency of the excitation laser.

Table I presents our final results for the center-of-gravity transition frequency f_{cog} and hyperfine coefficients A and B for the $6D_{5/2}$ state, as well as a comparison to previous results. The values are given from the center of gravity of the ground state to the center of gravity of the $6D_{5/2}$ state. The reported measurements were performed from both the $F = 3$ ground

state and the $F = 4$ ground state as a redundancy check of the results. The results from the two ground-state hyperfine levels are consistent with each other. Table II summarizes the statistical and systematic uncertainties.

IV. CONCLUSION

In this paper, we performed two-photon spectroscopy on the $6D_{5/2}$ state in neutral cesium-133. To our knowledge, the last absolute measurement of the $6D_{5/2}$ state was performed by Eriksson *et al.* in 1964 [10]. Our result improves

upon the measurement of Eriksson *et al.* [10] by a factor of 170 and will correct a 2.4σ discrepancy in the NIST database. A future measurement of this transition in an ultra-high-vacuum cell to eliminate possible pressure shifts could further reduce the uncertainty on the absolute transition frequency.

ACKNOWLEDGMENTS

This work was supported by the National Science Foundation through Grant No. PHY-1555232.

-
- [1] BIPM, *Le Système international d'unités / The International System of Units (The SI Brochure)*, 9th Edition (Bureau International des Poids et Mesures, Sèvres, France, 2019), <https://www.bipm.org/en/publications/si-brochure>, accessed 28 September 2021.
- [2] D. B. Newell and E. Tiesinga, *The International System of Units (SI): 2019 Edition, Special Publication (NIST SP)* (National Institute of Standards and Technology, Gaithersburg, MD, 2019).
- [3] V. Gerginov, K. Calkins, C. E. Tanner, J. J. McFerran, S. Diddams, A. Bartels, and L. Hollberg, *Phys. Rev. A* **73**, 032504 (2006).
- [4] V. Gerginov, C. E. Tanner, S. A. Diddams, A. Bartels, and L. Hollberg, *Opt. Lett.* **30**, 1734 (2005).
- [5] P. Fendel, S. D. Bergeson, T. Udem, and T. W. Hänsch, *Opt. Lett.* **32**, 701 (2007).
- [6] Y.-W. Liu and P. E. G. Baird, *Appl. Phys. B* **71**, 567 (2000).
- [7] J. Li, Z. Yi-Chi, X. Shao-Shan, W. Li-Rong, M. Jie, Z. Yan-Ting, X. Lian-Tuan, and J. Suo-Tang, *Chin. Phys. Lett.* **30**, 103201 (2013).
- [8] J. Deiglmayr, H. Herburger, H. Saßmannshausen, P. Jansen, H. Schmutz, and F. Merkt, *Phys. Rev. A* **93**, 013424 (2016).
- [9] W. D. Williams, M. T. Herd, and W. Hawkins, *Laser Phys. Lett.* **15**, 095702 (2018).
- [10] K. B. Eriksson, I. Johansson, and G. Norlén, *Ark. Fys.* **28**, 233 (1964).
- [11] J. E. Sansonetti, *J. Phys. Chem. Ref. Data* **38**, 761 (2009).
- [12] T.-J. Chen, J.-E. Chen, H.-H. Yu, T.-W. Liu, Y.-F. Hsiao, Y.-C. Chen, M.-S. Chang, and W.-Y. Cheng, *Opt. Lett.* **43**, 1954 (2018).
- [13] T. Ohtsuka, N. Nishimiya, T. Fukuda, and M. Suzuki, *J. Phys. Soc. Jpn.* **74**, 2487 (2005).
- [14] A. Kortyna, N. A. Masluk, and T. Bragdon, *Phys. Rev. A* **74**, 022503 (2006).
- [15] A. Kramida, Y. Ralchenko, J. Reader, and NIST ASD Team, *NIST Atomic Spectra Database (version 5.8)* (National Institute of Standards and Technology, Gaithersburg, MD, 2020), <https://physics.nist.gov/asd>, accessed 28 September 2021.
- [16] C. Patterson, A. Vira, M.-T. Herd, W. Hawkins, and W. Williams, *Rev. Sci. Instrum.* **89**, 033107 (2018).
- [17] J. I. Thorpe, K. Numata, and J. Livas, *Opt. Express* **16**, 15980 (2008).
- [18] E. C. Cook, A. D. Vira, C. Patterson, E. Livernois, and W. D. Williams, *Phys. Rev. Lett.* **121**, 053001 (2018).
- [19] E. C. Cook, A. D. Vira, and W. D. Williams, *Phys. Rev. A* **101**, 042503 (2020).
- [20] R. W. P. Drever, J. L. Hall, F. V. Kowalski, J. Hough, G. M. Ford, A. J. Munley, and H. Ward, *Appl. Phys. B: Photophys. Laser Chem.* **31**, 97 (1983).
- [21] N. P. Georgiades, E. S. Polzik, and H. J. Kimble, *Opt. Lett.* **19**, 1474 (1994).
- [22] C.-M. Wu, T.-W. Liu, M.-H. Wu, R.-K. Lee, and W.-Y. Cheng, *Opt. Lett.* **38**, 3186 (2013).
- [23] K.-H. Chen, C.-M. Wu, S.-R. Wu, H.-H. Yu, T.-W. Liu, and W.-Y. Cheng, *Opt. Lett.* **45**, 4088 (2020).